NASA Contractor Report 195478
AIAA–95–2968

A Transient Model of the RL10A–3–3A Rocket Engine

Michael P. Binder
NYMA, Inc.
Engineering Services Division
Brook Park, Ohio

June 1995

Prepared for
Lewis Research Center
Under Contract NAS3–27186

National Aeronautics and
Space Administration

A Transient Model of the RL10A-3-3A Rocket Engine

Michael Binder
NYMA, Inc.
2001 Aerospace Parkway
Brook Park, Ohio 44129

Abstract

RL10A-3-3A rocket engines have served as the main propulsion system for Centaur upper stage vehicles since the early 1980's. This hydrogen/oxygen expander cycle engine continues to play a major role in the American launch industry. The Space Propulsion Technology Division at the NASA Lewis Research Center has created a computer model of the RL10 engine, based on detailed component analyses and available test data. This RL10 engine model can predict the performance of the engine over a wide range of operating conditions. The model may also be used to predict the effects of any proposed design changes and anticipated failure scenarios. In this paper, the results of the component analyses are discussed. Simulation results from the new system model are compared with engine test and flight data, including the start and shut-down transient characteristics.

1.0 Introduction

The RL10A rocket engine is an important component of the United States space infrastructure. Two RL10 engines form the main propulsion system for the Centaur upper stage vehicle, which boosts commercial, scientific, and military payloads from a high altitude into Earth orbit and beyond (planetary missions). The Centaur upper stage is used on both Atlas and Titan launch vehicles. The initial RL10A-1 was developed in the 1960's by Pratt & Whitney (P&W), under contract to NASA. The RL10A-3-3A, RL10A-4, and RL10A-4-1 engines used today incorporate component improvements but have the same basic configuration as that of the original RL10A-1 engine. RL10's have been highly reliable servants of America's space program for over 30 years. The RL10A-3-3A engine is represented schematically in Figure 1.

The Space Propulsion Technology Division (SPTD) at the NASA Lewis Research Center began developing a computer model of the RL10 in 1991. This model was intended for government use in engine system research, mission-analysis and flight failure investigations. The first version of the model was created using data provided by Pratt & Whitney, and the ROCket Engine Transient Simulator (ROCETS) [1] system analysis program. This model could accurately predict the steady-state performance of the RL10A-3-3A, but the predicted time required for the engine to reach a specified thrust during engine start (time-to-accelerate) showed significant differences with test data [2]. It is believed that these discrepancies were due to errors in extrapolating the available component performance data to cover engine-start conditions, as well as errors in the physical models used for heat transfer and two-phase flow. Analysis of each RL10 engine component was undertaken in order to verify the origin of the data provided by P&W, and to improve the accuracy of the models at far off-design conditions. These analyses were also used to benchmark our ability to accurately model new rocket engine designs for which test data are not yet available; the RL10 engine system provided test data to validate the available component and system modeling tools.

In this paper, the RL10A-3-3A rocket engine and its various components are described briefly. The analysis results for each component are then discussed, including comparisons with existing component test data. The new engine system model, which includes the results of selected component analyses, is described and predictions of the model are compared to ground-test and flight data. For a more detailed discussion of the modeling work summarized here, the reader is referred to

the RL10A-3-3A Rocket Engine Modeling Project Final Report [3].

As the simulation results will show, the new RL10 model correctly predicts variation in engine transient behavior due to inlet conditions, initial thermal conditioning, and ignition delay.

2.0 RL10A-3-3A Engine Description

The RL10 engine design (all models) is based on a full expander cycle, as shown in Figure 1. Hydrogen fuel is used to cool the thrust chamber and nozzle, and the thermal energy transferred to the coolant is used to drive the turbopumps. Warm hydrogen gas is injected with cryogenic liquid oxygen into the combustion chamber and burned to provide thrust. During engine start, fuel tank pressure and the initial ambient heat in the cooling jacket metal are used to start rotation on the turbine. After ignition, the heat of combustion is used to accelerate the turbopumps to full power. Because the Centaur upper stage vehicle uses two RL10 engines, it is important that the engines start simultaneously (to minimize thrust imbalances). For the purpose of providing a quantitative measure of the engine start times, we shall refer to the time between the start signal and the chamber pressure reaching 200 psia as the *time-to-accelerate*.

During engine shutdown, the fuel inlet, fuel shut-off, and oxidizer inlet valves are closed. The combustion process stops and the fuel and oxidizer drain from the engine system; LOX drains out through the thrust chamber, and the fuel drains out through the pump cool-down valves.

3.0 Turbomachinery Analysis

3.1 Turbopump Background Information

The RL10A-3-3A turbopump includes a two-stage fuel turbine which drives a two-stage fuel pump on a common shaft, and a single-stage LOX pump through a gear box. At the engine's normal operating point, a fuel flow of 6 lb/sec is pumped to a pressure of 1100 psia, and 30 lb/sec of LOX is pumped to 600 psia. The normal operating speed of the fuel pump is 32000 rpm, and the LOX pump speed is 12800 rpm.

Pratt & Whitney provided the NASA SPTD with test data maps of head coefficient and efficiency for each pump stage as functions of flow coefficient, and included a speed correction factor for efficiency. These maps do not cover the entire range of operating conditions experienced by the pumps during engine start and shutdown. P&W had also provided the SPTD with test data maps of turbine efficiency and flow resistance as functions of overall pressure ratio and velocity ratio (u/c_0). These maps do cover a range of conditions suitable for engine start and shutdown simulations.

3.2 Detailed Pump Analyses

Two different analysis codes, PUMPA [4] and LSISO [5], were used to model the RL10A-3-3A fuel and LOX pumps. The pump head coefficients predicted by each code agree with test data to within five percent (5%) over the engine's normal steady-state operating range. The PUMPA and LSISO efficiency predictions, however, differed from test data by as much as fifteen percent (15%), and could therefore not be used in the engine system model. PUMPA was also used to predict the performance of the RL10A-3-3A pumps at the engine start conditions. The results of these analyses were used qualitatively to help extrapolate the head maps beyond the available test data provided, as discussed later in this section. It should be noted that a subsequent version of the PUMPA code was recently developed which better predicts the RL10A-3-3A pump design point efficiency, without affecting the head predictions. The new version of PUMPA was completed too late to allow a comprehensive analysis of start conditions to be performed again for this project.

In addition to the PUMPA and LSISO analyses described above, a third analysis was performed which was specifically designed to estimate the low speed pump head (as experienced during start). This method was suggested by Rostafinski [6] and requires that the design point performance of the pump be known. This approach, when combined with a separate model of the pump exit diffuser, appears to match well with the limited test data available at engine start conditions. Although promising, this modeling technique proved impractical for transient system simulation (slow execution, numerical instabilities, etc.) and was therefore not included in the new RL10 system model.

Using available engine test data and information gained from the analyses discussed above, the pump performance maps provided by Pratt & Whitney were extrapolated to include conditions at engine start and shutdown (zero speed, reverse flow, cavitation, etc.). In order to represent such a wide range of operating conditions, a map format suggested by Chaudhry [7] is used. The new map format defines normalized head parameter (h) and torque parameter (β) as functions of a third parameter, θ (theta) as described below. The new

pump performance maps for the engine system model are shown in Figures 2 and 3.

$$h = \frac{\left(\frac{\Delta H}{\Delta H_d}\right)}{\left(\left(\frac{Q}{Q_d}\right)^2+\left(\frac{N}{N_d}\right)^2\right)} \qquad \beta = \frac{\left(\frac{\tau}{\tau_d}\right)}{\left(\left(\frac{Q}{Q_d}\right)^2+\left(\frac{N}{N_d}\right)^2\right)}$$

$$\theta = \arctan\left(\frac{\left(\frac{N}{N_d}\right)}{\left(\frac{Q}{Q_d}\right)}\right)$$

where ΔH = head (in feet)
N = shaft speed (in rpm)
Q = volumetric flow (in gpm)
and the subscript d denotes the design condition.

The results of the pump analyses described above indicate that it should be possible to predict the general performance characteristics of new pump designs. Results from this type of analysis are valuable for conceptual engine design and simulation activities. Such component predictions may not be sufficiently accurate for use in engine start-transient simulations, especially if no test data is available with which to anchor the new pump models.

3.3 Detailed Analysis of Fuel Turbine

The RL10A-3-3A turbine was also analyzed using the TURBA code [8], which is currently being developed at the NASA Lewis Research Center. TURBA is a one-dimensional mean-line code which combines basic physics (velocity triangles and isentropic relationships) with empirical correlations derived from existing turbine designs. The turbine performance predictions could not be directly compared with the maps provided by P&W. Instead, both sets of maps were used as inputs to a simple turbine simulation, and the resulting overall efficiencies and flow rates were compared. Although the overall performance trends predicted by TURBA are similar to those indicated by the P&W data, a more quantitative comparison shows that significant differences exist. The predicted overall turbine efficiency, for example, differs by more than 5% from the P&W data, especially at low speeds. It has been further noted that relatively small variations in the turbine performance at low speeds can profoundly affect the RL10 engine time-to-accelerate. Possible explanations for the poor match between TURBA output and test data have not been explored; the TURBA code is still considered to be in the development phase. The performance maps provided by P&W have therefore been retained in the new system model.

The turbine analysis performed in this study indicates that it is possible to estimate the design point performance of a new turbine to within a few percent. It is also possible to predict the overall trends in performance at off-design conditions. As with the pump analyses discussed above, however, the accuracy of the turbine predictions may not be sufficient for use in transient or deep-throttling simulations of a new engine. When component test data is available for a new turbine design, it might be possible to adequately adjust the model based on only a few test data points.

4.0 Thrust Chamber and Cooling Jacket

4.1 Thrust Chamber Background Information

The walls of the RL10A-3-3A thrust chamber are constructed of stainless steel tubing. Hydrogen fuel is pumped through these tubes in order to cool the walls of the thrust chamber and provide thermal energy to the turbine. The tubes are brazed together and reinforced with bands on the outside, as well as a metal girdle around the throat section. A silver throat insert is cast in place to increase the nozzle area ratio and specific impulse. The thrust chamber normally operates at a pressure of 475 psia, a mixture ratio (O/F) around 5.0, a thrust of 16500 lbf, and a specific impulse of 445 seconds.

The analysis of the RL10A-3-3A thrust chamber was divided into three basic areas: 1) cooling jacket heat transfer, 2) combustion chamber performance, and 3) nozzle performance. Each analysis is described below.

4.2 Detailed Analysis of Cooling Jacket Heat Transfer

The original model of the RL10 cooling jacket had only five heat transfer calculation nodes distributed along the cooling circuit. This model was considered to be too coarse and a more detailed model was created for this project.

CET93, a one-dimensional equilibrium program [9], was used to refine the table of hot-gas properties. The Rocket Thermal Evaluator (RTE) code [10] was used to predict the flow resistance of the cooling jacket and the effects of tube curvature on heat transfer rate. Heat transfer between the combustion gas and chamber walls

was predicted using an enthalpy-driven Bartz correlation [11]. The enthalpy gradient was used instead of the temperature gradient because this more accurately predicts variation in heat transfer at different mixture ratios. A Colburn correlation [12] was used to determine the heat transfer from the chamber wall to the coolant flow. It was discovered that combining twenty hot-gas and metal property nodes with five (rather than 20) coolant nodes could significantly increase the computational efficiency of the transient system model without loss of accuracy overall. This the configuration was used in the new RL10A-3-3A system model.

Figure 4 shows the predicted heat flux, wall temperature, coolant temperature and pressure along the axial length of the thrust chamber cooling jacket. Test data showing axial variation in temperature and pressure are not available for comparison. The accuracy of the new heat transfer model can only be judged by the overall temperature rise and pressure drop across the cooling jacket. Based on these parameters, an empirical correction of 1.08 was added for the hot-gas heat transfer coefficient and a factor of 0.94 applied to the predicted jacket flow resistance. These empirical correction factors represent average values, since the actual heat transfer coefficient appears to vary somewhat from one RL10 engine to another. These variations may be due to small manufacturing differences; they are not considered critical as long as the engine has sufficient starting power.

A simple one-dimensional film boiling model was also added to the cooling jacket heat transfer model. Film-boiling effects have been suggested as the cause of the four to eight Hertz pressure oscillations often experienced during the RL10 engine start sequence. The new model still does not show these pressure oscillations; they may be due to two-dimensional effects not modeled here or to local choking within the two-phase fluid.

The analyses presented here demonstrate the capability of one-dimensional models to predict the effects of various conditions on heat transfer. Depending on the accuracy required for system simulations, some adjustment to the heat transfer coefficients using test data may be required. Test results are also useful in defining the variability in heat transfer characteristics due to manufacturing tolerances and other factors.

4.3 Detailed Analysis of Combustion Chamber Performance

In addition to revising the combustion gas property tables for the new model, several other improvements were made. In the original RL10 engine model, the thrust chamber was treated as a single point, without considering axial variation. In reality, there are momentum losses and changes in static pressure along the hot-gas flow path which will affect performance. These effects were relatively simple to predict and were added to the model. An analysis of the RL10A-3-3A thrust chamber assembly was also performed using the ROCCID code [13], which provides a capability of modeling the propellant injectors, atomization and combustion processes. The objectives of this analysis were to validate our capability to predict c*-efficiency using RL10 data from P&W, and to extend the range of mixture ratios represented in that data set. The RL10 injector proved difficult to model using ROCCID; several aspects of its design are not found in the more contemporary designs which ROCCID was intended to model. As a result, the results of the ROCCID analyses did not show a good match with the P&W data. The ROCCID model also experienced numerical convergence problems at low pressures (below 160 psia), where the c*-efficiency changes significantly. The data maps provided by P&W have been retained in the new system model.

During the engine start sequence, heat transfer in the injector can play a discernable role in the system's dynamic behavior, primarily by changing the density of the injected LOX. Simple models of heat transfer in the injector elements and inter-propellant bulkhead were added to the new engine model. Although there is insufficient test data to validate the models, the results appear reasonable. The addition of these modeled effects delays the time-to-accelerate by approximately 100 milliseconds. Considered over all engine start transients simulated, this delay results in a more accurate prediction of time-to-accelerate. Figure 5 shows the predicted heat transfer rate in the injector as a function of time during a typical engine start.

4.4 Detailed Analysis of Nozzle Performance

The RL10A-3-3A nozzle performance affects the combustion chamber pressure and flowrate, as well as the specific impulse and thrust of the engine. Pratt & Whitney had originally provided nozzle performance data in the form of specific impulse (Isp) tables with additional corrections for various kinetic losses. Analyses were performed at Lewis using a Two Dimensional Kinematics (TDK) program [14] in order to

better understand the P&W data. Figure 6 shows the output of the TDK analysis compared with the P&W data. The results match well at the engine's normal operating point of 475 psia and O/F = 5.0. The predicted and P&W values differ more significantly at low pressures and mixture-ratios, however. The predicted Isp maps have been included in the new RL10A-3-3A system model.

Several different approaches were taken to determine the nozzle discharge coefficient (Cd). P&W had specified a Cd of approximately 0.98. A Navier-Stokes analysis [15] was performed at Lewis which predicted the discharge coefficient to be 0.979, a remarkable agreement. Trimming the Cd value used in the engine simulation to match predicted chamber pressure with test data gave a value of 0.975. The TDK analysis described above had further indicated that the Cd may change somewhat with chamber pressure and mixture ratio. After considering these various results, a constant Cd of 0.975 was selected for use in the new system model.

5.0 Miscellaneous Components

In general, the ducts, valves, and manifolds in the RL10 engine were not analyzed in detail. Many of these components have complex geometries that would require finite-element methods to model properly. In the case of the fuel pump cool-down valves, oxidizer control valve, and LOX injector elements, however, the models for two-phase flow contained in the original model required improvement. We also attempted to verify the resistance of a single duct as specified by Pratt & Whitney using generic one-dimensional methods.

During the engine start, several components experience two-phase critical and unchoked flow conditions. The fuel-pump cool-down valves, which vent liquid hydrogen overboard, are always choked and the hydrogen flashes to vapor as it is vented. The oxidizer control valve and LOX injector elements experience two-phase flow for only a small period of time during start, transitioning at some point between choked and unchoked conditions. The challenge was to devise models which allow a relatively continuous transition between the various flow conditions during start.

A number of different approaches were considered [16] [17] [18]. Ultimately, a model was derived which treats the flow as incompressible, but limits the assumed downstream pressure to either saturation or isentropic critical pressure, depending on the value of the pressure upstream of the orifice or valve. This modeling approach was used for the LOX injector elements and fuel cool-down valves. Two-phase flow in the oxidizer control valve is modeled as incompressible, limited by the saturation pressure of the fluid until the flow becomes entirely gaseous, after which it is treated as isentropic flow of an ideal gas. These models agree well with available test data.

The fluid resistances of ducts and tubes are typically determined by flow testing those components. For proposed new rocket engine systems, empirical data of this kind may not be available during the analysis phase. A simple one-dimensional analysis[19] of flow in an RL10 duct (from the turbine discharge to the main fuel shut-off valve) was performed and the results were compared with the resistance specified by P&W. The surface roughness on the interior of the duct was not known, so we considered a range of options from smooth commercial steel pipe to drawn tubing. The analyses indicated a range of possible K values[19] from 0.928 to 0.487; the value of K given by P&W was 0.648. Our estimates therefore define a range of possible values which bracket the suggested value with an error of 25 to 43 %. The resistance provided by P&W has been retained for the new RL10 engine model, but this analysis suggests that we can probably estimate the resistance for a new (untested) duct to within +/- 30%. Better estimates might be possible if the surface roughness of the intended duct is well defined.

It is evident from the discussion above that accurate one-dimensional models of ducts and valves in a new engine design will require at least some flow testing. Before such data is available, it would be prudent to consider the effects of uncertainty in engine system simulations. In the case of valves and ducts where two-phase flow might exist, it is advisable to test the components over their entire operating range, since two-phase effects can often lead to unexpected behavior. Flow models which include two and three dimensional effects may also produce more accurate resistance predictions.

6.0 New RL10A-3-3A Engine System Model

The new RL10A-3-3A engine system model includes the results of several of the detailed component analyses, as described above. In addition to these component model changes, several improvements were made in the structure of the system model itself. Tracking of the total-to-static conversions for pressure

and enthalpy was improved in the new system model, for example.

It became necessary to create two different models of the RL10 engine: one for simulating start transient behavior and steady-state performance, and the other for simulating shut-down transient behavior. During shut-down, the ducts and manifolds in the engine are emptied into space, and dynamic volumes had to be added to the model to allow the simulation of these effects. Including these dynamic volumes in the start transient and steady-state model changed the predicted start transient behavior significantly, in disagreement with test data. These differences could not be resolved, and so two separate models were developed.

6.1 Effects of Modeling Uncertainty

Before discussing the output of the new system model, it is important to note several unresolved sources of uncertainty in the model which will affect our ability to accurately simulate a given RL10 engine firing. These uncertainties can be divided into four categories: 1) uncertainty in hardware characteristics, 2) uncertainties in valve dynamic behavior, 3) uncertainties in engine initial conditions, and 4) uncertainty in the main chamber ignition delay. There is also a great deal of non-linear interaction between RL10 engine components [20]. Characterizing the interaction between the various operating parameters with uncertainty was beyond the scope of this study.

6.1.1 Uncertainties in Hardware characteristics

There is some uncertainty in the actual value of the discharge coefficient for the fuel-pump cool-down valves. In the RL10 model, the discharge coefficient is set at 0.6 for ground-test and 0.8 for flight. These values were chosen based on discussions with engineers at Pratt & Whitney but no real calibration data is available to verify these values. The resistance of the cool-down valves is an important factor in the engine time-to-accelerate.

The drag torque (due to bearings, seals, gears, etc.) of the RL10 turbopump (fuel and LOX combined) is a known source of engine-to-engine variation. The value is not generally measured for each engine but past studies have shown that the torques vary from 8 to 36 lbf-in (with respect to the fuel pump shaft)[20]. A constant nominal value of 20 lbf-in has been used for all simulations run for this study. It is uncertain what the actual values of running torque were for the test and flights considered but it is unlikely that the values were all precisely 20 lbf-in.

6.1.2 Uncertainties in Valve movement

The transient behavior of the engine in both start and shutdown is largely determined by the opening and closing of valves. Variations in valve and actuator behavior actually do occur for a variety of reasons. In some cases, the opening and closing times of valves can be inferred from test data. In most cases, however, this is not possible because of the limited number of engine sensors and their dynamic response rates. Valve data provided by P&W has been combined with information inferred from available test data to define 'typical' valve movement schedules for the new system model. This single set of typical schedules was used for all simulations performed in this study.

6.1.3 Uncertain Initial conditions

The temperature of the combustion chamber, nozzle and cooling jacket at the beginning of the engine start sequence is an important factor in the engine time-to-accelerate. Unlike the engine inlet pressures and temperatures, there is no reliable measurement of initial jacket temperature for any given test or flight. Temperatures that are measured on the engine generally show false readings before start due to ambient conditions, metal conduction with other components, and the lack of propellant flow at that time. The initial temperature of the cooling jacket, ducts, manifolds, and other components must be estimated, often based on limited information from past testing.

In the RL10 model discussed here, the temperature of the cooling jacket is assumed to be a uniform 540 R for first burns and 350 R for second burns. The cooling jacket inlet manifold is assumed to be at 200 R because the inlet manifold is exposed to some of the fuel pump cool-down flow before start. All other components in the system are assumed to be in thermal equilibrium with the propellant flows at start. Because these assumptions are somewhat arbitrary, they are likely to be in error to some degree for any given firing.

6.1.4 Uncertainty in Ignition delay

For the simulations considered here, the ignition times were set manually to agree with the measured data. In order to simulate an engine start for which data is not yet available, a model of the ignition process would be required. This model could be

based on theoretical analysis, or might be derived from test data. NASA does not currently have an ignition model for the RL10.

6.2 RL10 Steady-state Engine Performance Predictions

Ten test cases are considered for the steady-state performance predictions. Five tests are based on different quiescent operating points for a single ground-test run of a single engine (Engine P2087, Run 2.01, October 4,1991). The other five tests are based on the final states of five start-transient data sets (five different ground-test runs) of a single engine (P2093). Flight data has not been included in this comparison because insufficient data exists to determine the mixture-ratio and trim position of the oxidizer control valve (OCV) for those firings. For the ground-test runs considered, the OCV position has been trimmed in the simulation to achieve the steady-state mixture ratio indicated by the test data. Since the OCV position is not a measured parameter, the simulated trim position could not be verified directly with test data. A comprehensive performance prediction for a typical case is shown in Table 1. In general, only a few parameters are actually measured on engine firings (14 parameters on ground-tests, 8 in flight). Of the fourteen parameters measured in ground-tests, five are used as inputs to the model (inlet conditions and chamber pressure), and so only nine predicted parameters are compared with test data for each case.

Figure 7 shows the distribution of error between the measured and predicted parameter values in the ten ground-test cases. The model predictions match the measured values to within 10% for all parameters on all tests (a total of 90 values). Most predictions are within 3% of the test results. The most significant errors are in the turbine inlet temperature and the pump discharge pressures. The difference between the predicted and measured turbine inlet temperature varies from engine to engine, as discussed in section 4.2 of this paper. The error in the pump discharge pressures appears to be associated with turbopump speeds that are consistently lower than measured. This discrepancy in speed is most likely due to small errors in the turbine maps and cooling jacket model; these errors cannot be easily corrected for without adversely affecting the predicted start behavior. The turbine performance maps provided by P&W for transient simulation are not the same as those originally provided for use in the steady-state model. The original maps do not work well in simulating the start transient but the new maps do not match as well at the engine's design operating conditions. The new system model's steady-state predictions are therefore slightly less accurate than those of the original system models. It was decided, however, that the turbine maps suggested for start transient modeling would be used throughout, and the associated steady-state error accepted.

6.3 RL10 Start Transient Simulations

The results of RL10 start transient simulations were compared with both ground-test and flight data. Figure 8 (a - e) shows the predicted and measured start transients of a single ground-test first-burn. Figure 9 shows chamber pressure and pump speed data for an Atlas/Centaur flight (AC-72), while Figure 10 shows similar data for the second burn (restart) of a different flight (AC-74). In each of these runs, the ignition time has been set in the model based on examination of the test or flight data. The difference between ground-test and flight engine simulations is the value chosen for the fuel cool-down valves discharge coefficient (which reflects differences between the vehicle and test-stand ductwork). The difference between first and second burn simulations is the assumed initial temperature of the combustion chamber metal. These assumed variations were also discussed in section 6.1 above.

The start model generally matches the measured time-to-accelerate of the engine to within approximately 230 milliseconds, using only estimates for initial temperatures, bearing friction, valve schedules and other factors which may vary from run to run and from engine to engine. Table 2 gives the predicted vs. measured time-to-accelerate for six ground-test and three flight-engine firings. One of the flight simulations is off by 280 msec (rather than 230 msec), but this appears to be an aberration relative to other flight-engine starts. Comparing the results of this start transient with those from other flights, it appears likely that the conditions for this flight were different in ways other than their inlet conditions alone. The model correctly predicts start variations due to different engine inlet conditions, initial thermal conditions, and differences between ground and flight hardware.

The reader may note from Figures 8-10 that there are some transient differences between the predicted and measured chamber pressures which occur after the engine bootstraps but before it reaches the quiescent state. The small oscillations evident in the test data are due to oscillations of the Thrust Control Valve (TCV) servo-mechanism. The simulation does not include a model of the actuator dynamics, but the TCV is assumed to open as a simple linear function of

combustion chamber pressure. The simulation therefore overshoots the desired chamber pressure and does not oscillate. In several cases, the simulation does show some unusual transients before reaching steady-state; these appear to be due to volume dynamics in the LOX pump inlet duct. As the OCV suddenly opens and the LOX system pressurizes, the simulation predicts oscillations caused by fluid compression, inertia, and phase changes. These transients, which are not evident in the test data, may occur in the simulations because OCV servo dynamics are not included in the model. These transient differences between prediction and test are not considered significant; they would be minimized if models of the TCV and OCV actuators are developed in the future.

To demonstrate one potential application of the system start model, Figure 11 shows the predicted metal temperature of the combustion chamber just upstream of the throat (its hottest point). This parameter is not measured, even in ground tests. The temperature in this case peaks at around 1875 R, which is a few hundred degrees below the melting point of the silver throat insert. Information of this kind can be used to help determine component wear and to assess the impact of operational or hardware changes to the engine.

6.4 RL10 Shutdown Transient Simulations

Two firings have been used for comparison between model predictions and measured data. RL10 engine shutdowns do not appear to have any distinct feature analogous to the time-to-accelerate for start transients. Although there are subtle variations in the rate of deceleration, the nature of these differences is not as well understood as in the case of engine start.

Figure 12 (a-d) shows the predicted vs. measured shutdown for a ground-test engine. The RL10 shutdown model has captured many interesting effects that occur during shutdown. In Figure 12c, for example, the simulated and measured venturi pressures both show a characteristic dip, rise and then falloff in the fuel venturi upstream pressure. This feature is caused by the dynamic interaction of the fuel pump cool-down valve opening and main fuel shutoff valve closing. Another interesting characteristic of the RL10 shutdown transient (as shown in Figure 12c) is the jump in fuel pump inlet pressure due to reverse flow through the fuel pump.

7.0 Concluding Remarks

The major goals set for this project were to create a transient model of the RL10A-3-3A rocket engine for government use, to better understand the engine and its components, and to benchmark the available component analysis tools using an existing engine design. These goals have been accomplished.

The new RL10 start transient model accurately predicts the engine time-to-accelerate when compared to ground-test and flight data. The model can simulate engine start transients over a wide range of inlet conditions, initial thermal conditions, and ignition delays. This model also predicts steady-state performance values which are within 10% of the measured values in all cases, and within 3% for most parameters. The new RL10 shutdown model successfully reproduces the engine's transient behavior after main engine cut-off. These new system models could be used in the future to predict the effects of changes in the engine design, and to simulate off-nominal operating conditions.

In performing the detailed component analyses described in this paper, a great deal has been learned about the RL10 engine. This activity has also provided an opportunity to compare the output from available component modeling tools with test data from an existing engine design. Comparison of the analysisresults with data provided by Pratt & Whitney indicates that at least some empirical correction must be made to the results of the component models. Such component models are nonetheless valuable in predicting the off-design characteristics of the engine components, especially once empirical corrections have been included. Detailed three-dimensional computational-fluid-dynamic models may also be considered in the future to improve the accuracy of component performance predictions, though even such advanced techniques will involve some uncertainty, especially for new component designs. The capability may not yet exist to precisely predict the behavior of new components or engines for which no test data is available. In such cases, the best that can be expected is to define a range of performance and transient behavior based on analysis. This type of information can be extremely valuable in the design and development of new components or systems, especially in combination with probablistic and uncertainty analysis techniques.

Acknowledgements

This work was performed under contract NAS3-27186.

The author would like to acknowledge the participation of the following individuals, who performed the component analyses which were incorporated into the new RL10A-3-3A system model.

Tom Tomsik (NASA LeRC) - Heat Transfer
Joseph Veres (NASA LeRC) - Turbine and Pumps
Ken Kacynski (NASA LeRC) - Combustion and Nozzle
Doug Rapp (Sverdrup / NYMA) - Hot gas properties
Dean Scheer (Sverdrup / NYMA) - Pumps
Albert Pavli (Sverdrup / NYMA) - Injector
William Tabata (NASA LeRC) - General RL10 information and expertise.

Pratt & Whitney (West Palm Beach, Florida) also participated in this work, supplying us with design information and test data for validation.

References

1. **Pratt & Whitney Government Engines, *System Design Specification for the ROCETS System - Final Report*, NASA CR-184099, July 1990.**

2. **Binder, M. - Sverdrup Technology Inc., *An RL10A-3-3A Rocket Engine Model Using the ROCETS Software*, AIAA Paper 93-2357, June 1993.**

3. **Binder, M., Tomsik,T., Veres,J., *RL10A-3-3A Modeling Project - Final Report*, NASA TM (number pending), 1995.**

4. **Veres, J., *A Pump Meanline Analysis Code (PUMPA)*, NASA TM-106745, October 1994.**

5. **Gulbrandsen, N. *Centrifugal Pump Loss Isolation Program (LSISO)*, COSMIC Program # MFS-13029, April 1967. *(note that the version of LSISO used in this study is not publicly available, this reference gives a general description of the program in its original, publicly disseminated form).**

6. **Rostafinski, W., *An Analytical Method for Predicting the Performance of Centrifugal Pumps During Pressurized Startup*, NASA TN D-4967, January 1969.**

7. **Chaudhry,H., *Applied Hydraulic Transients - 2nd Edition*, Van Nostrand Reinhold, New York 1987.**

8. **Veres, J., *A Turbine Meanline Analysis Code (TURBA)*, NASA TM (number pending), 1995.**

9. **McBride,B. and Gordon,S. *CET93 and CETPC: An Interim Updated Version of the NASA Lewis Computer Program for Calculating Complex Chemical Equilibria with Applications* , NASA TM-4557, March 1994.**

10. Naraghi, M.H.N., *RTE - A Computer Code for Three-Dimensional Rocket Thermal Evaluation*, (NASA Grant NAG 3-892), July 1991.

11. Bartz, D.R., *Survey of Relationships between Theory and Experiment for Convection Heat Transfer in Rocket Combustion Gases*, Advances in Rocket Propulsion, AGARD, Technivision Services, Manchester, England, 1968.

12. Holman,J.P., *Heat Transfer - Fourth Edition* McGraw Hill, 1976

13. Muss, J. and Nguyen,T., *User's Manual for Rocket Combustor Interactive Design (ROCCID) and Analysis Computer Program*, NASA CR-1087109, May 1991.

14. Nickerson,G., *Two-Dimensional Kinetics (TDK) Nozzle Performance Computer Program - Users Manual*, (NASA Contract NAS8-39048), March 1993.

15. Kacynski, K., *Calculation of Propulsive Nozzle Flowfield in Multidiffusing, Chemicallyreacting Environments*, NASA TM 106532, 1994.

16. Henry, R. and Fauske, H., *The Two-phase Critical Flow of One-Component Mixtures in Nozzles, Orifices, and Short Tubes*, ASME Journal of Heat Transfer, May 1971.

17. Applied Physics Laboratory, *JANNAF Rocket Engine Performance Test Data Acquisition and Interpretation Manual*, CPIA Publication 245, April 1975.

18. Simoneau, R. and Hendricks, R., *Generalized Charts for the Computation of Two-phase Choked Flow of Simple Cryogen Fluids*, Cryogenics, February 1977.

19. Crane Co. and ABZ Inc., *Crane Companion to Flow of Fluids Through Valves, Fittings, and Pipe*, (software), 1992.

20. RL10 Start Capability Working Group (government/industry cooperative), *AC-71 Failure Investigation - Final Report*, (no contract or report number given), December 1993.

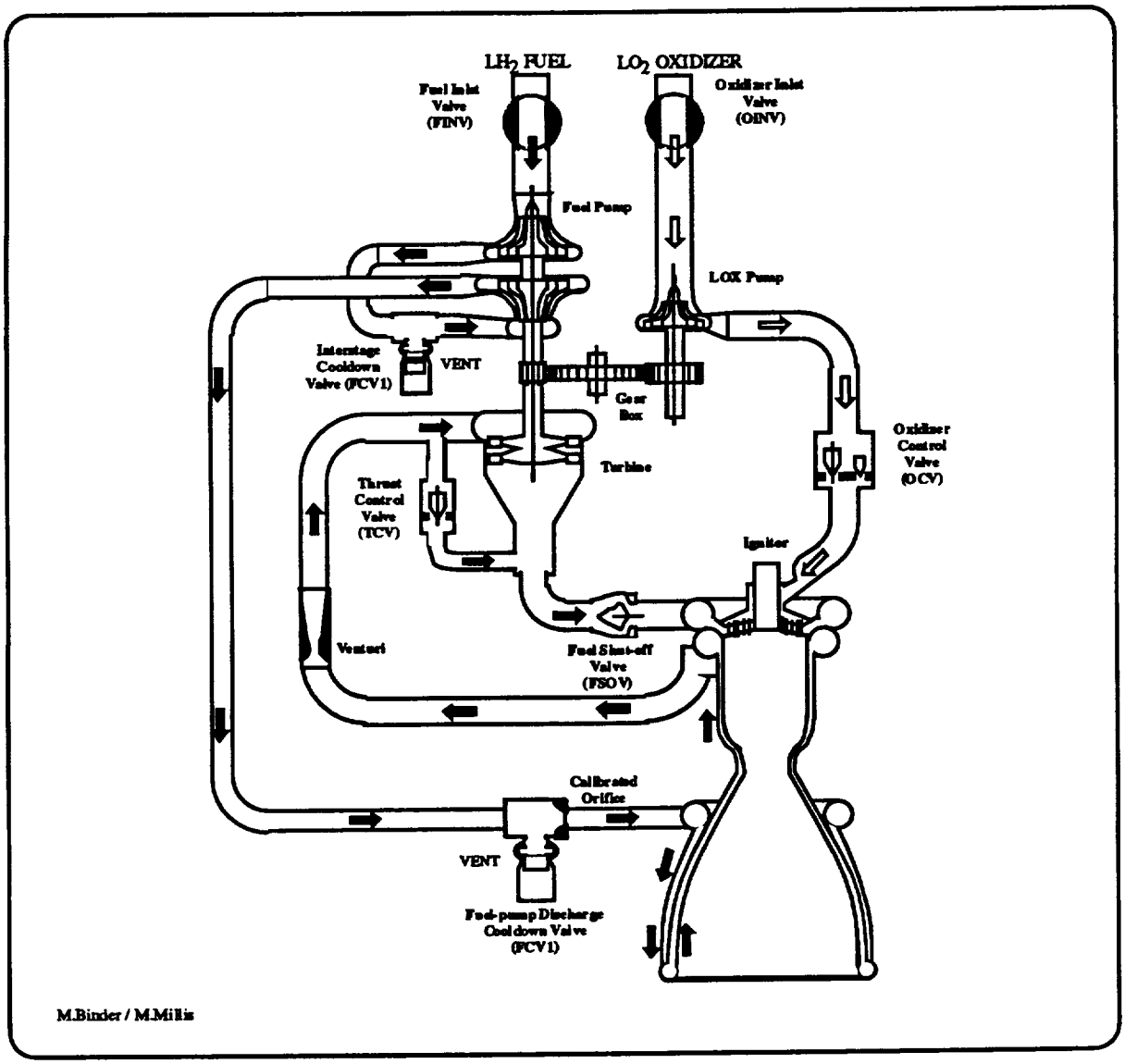

Figure 1
RL10A-3-3A Engine System Schematic

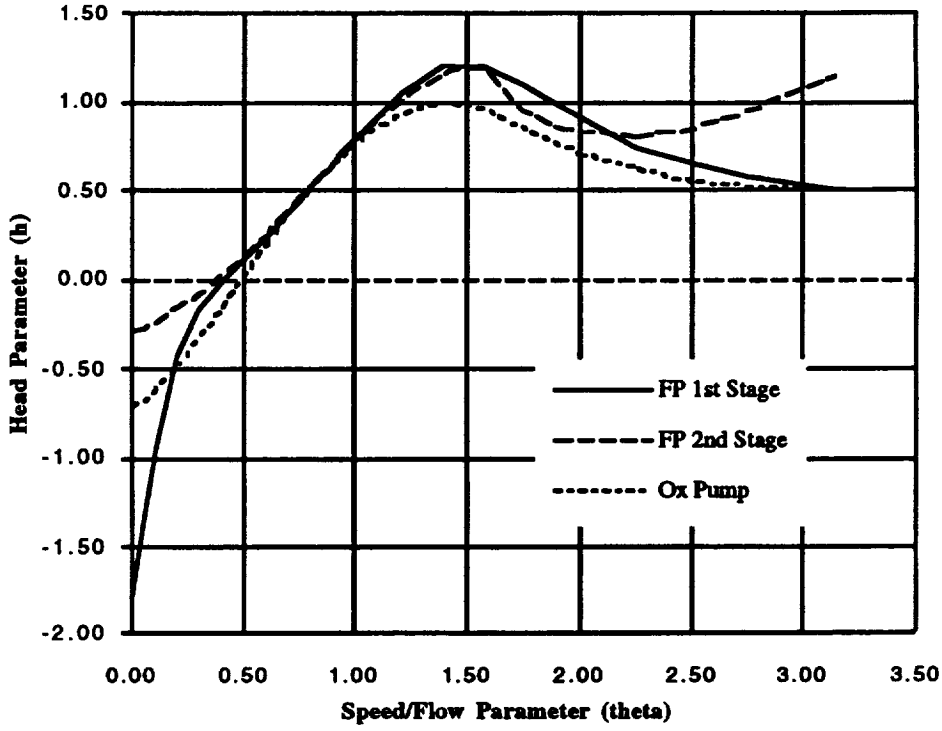

Figure 2
Extrapolated Pump Head Maps for RL10 Model

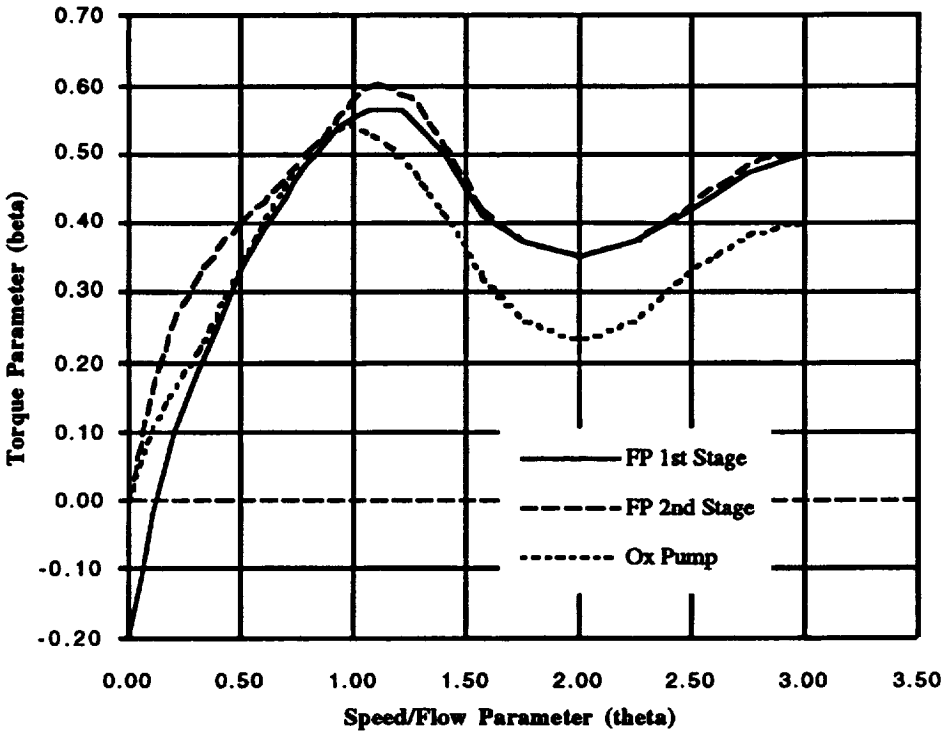

Figure 3
Extrapolated Pump Torque Maps for RL10 Model

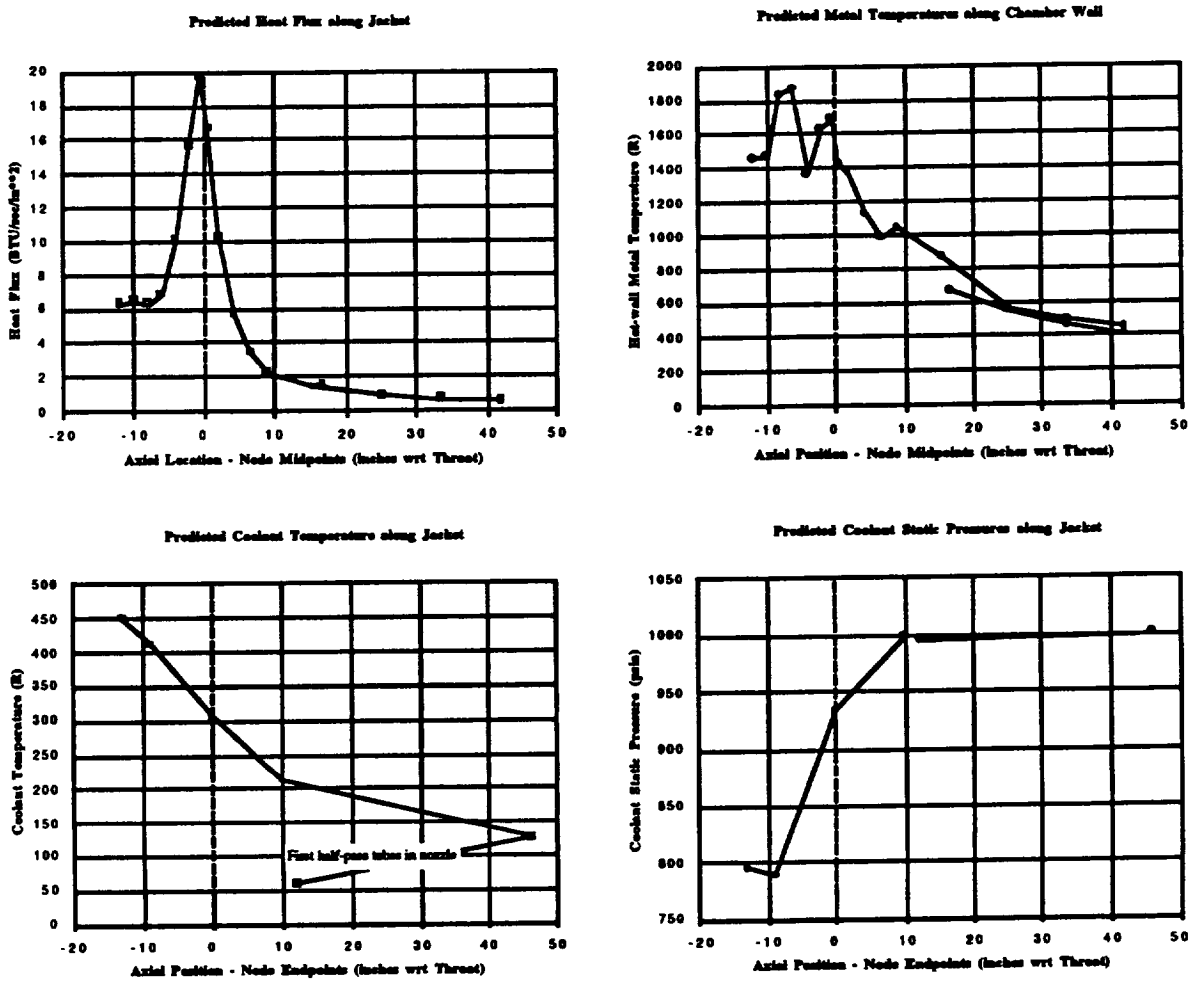

Figure 4
Predicted Axial Variation in Heat Transfer with New Model

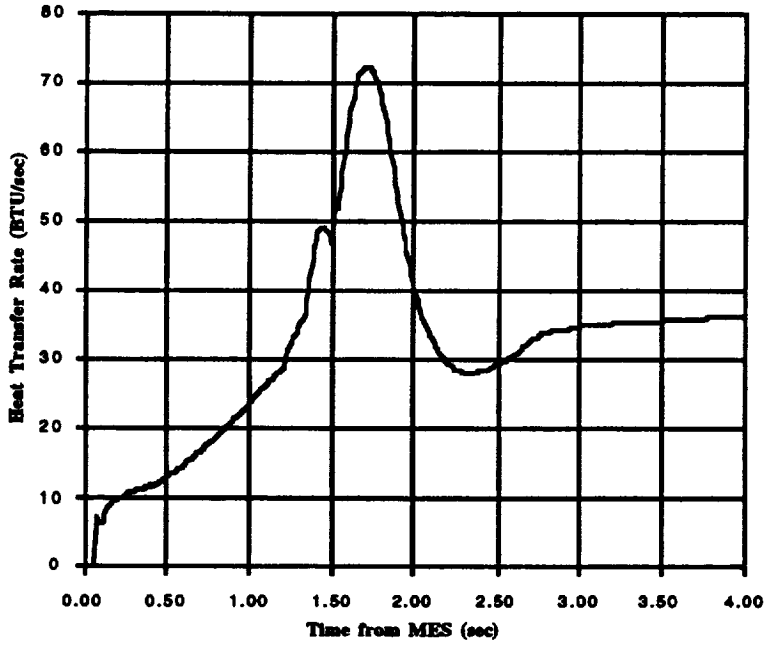

Figure 5
Predicted Heat Transfer in Injector Plena during Engine Start

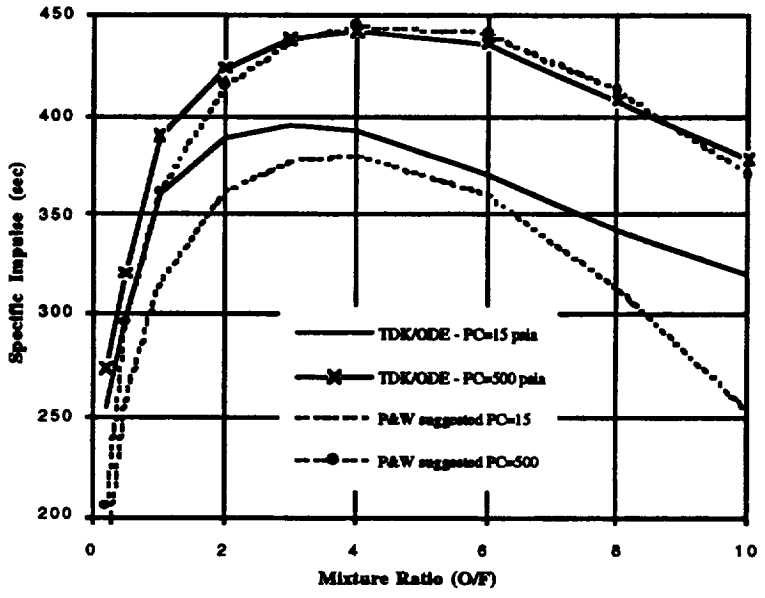

Figure 6
TDK/ODE Predictions of Isp vs. P&W Suggested Values

OVERALL ENGINE PERFORMANCE

Chamber Pressure (at injector face)	475.5	psia
Engine Thrust	16412	lbf
Engine Inlet O/F	4.993	
Combustion O/F	5.055	
Specific Impulse	445.6	sec
Fuel Consumption	6.161	lb/sec
Oxidizer Consumption	30.76	lb/sec

COMBUSTION CHAMBER / NOZZLE

Nozzle Stagnation Pressure	473.5	psia
Combustion Temperature	5816	R
c* Efficiency	0.9892	
c* (ideal)	93885	in/sec
Engine Exit Pressure (ambient)	0.01	psia
Fuel-LOX heat transfer at injector	40.36	BTU/sec

FUEL-SIDE ENGINE CONDITIONS

Location	static pressure (psia)	total pressure (psia)	total temp (deg R)	mass flow (lb/sec)	density (lb/cu.ft)	total enthalpy (BTU/lb)
Fuel Tank	27.68	27.68	38.60	.....	4.337	-105.1
Fuel Pump Inlet	26.08	27.19	38.6	6.161	4.337	-105.1
Fuel Pump Interstage	532.2	534.8	47.65	6.118	4.285	-68.21
Fuel Pump Discharge	1058.9	1067.3	57.63	6.082	4.220	-27.84
Cooling Jacket Inlet	1018.3	1026.6	57.94	6.082	4.185	-27.84
Cooling Jacket Exit	816.8	830.9	384.2	6.082	0.3855	1240.5
Turbine Inlet	796.7	813.8	384.2	6.056	0.3767	1240.5
Turbine Hiusing Exit	562.2	576.2	361.1	6.082	0.2868	1149.2
Fuel Injector Plennum	537.9	537.9	359.4	6.082	0.2742	1142.4
Chamber	475.5					

OXIDIZER-SIDE ENGINE CONDITIONS

Location	static pressure (psia)	total pressure (psia)	total temp (deg R)	mass flow (lb/sec)	density (lb/cu.in)	total enthalpy (BTU/lb)
Oxygen Tank	42.35	42.35	174.7	.....	69.07	66.42
Ox Pump Inlet	36.33	39.96	174.7	30.76	69.07	66.42
Ox Pump Discharge	601.5	621.1	178.6	30.75	69.02	68.84
Oxid. Injector Plennum	529.4	539.3	182.1	30.75	68.31	70.15
Chamber	475.5					

TURBOMACHINERY PERFORMANCE

	delta-Head (feet)	Volume Flow (gpm)	Speed (rpm)	Torque (lbf-in)	Efficiency
Fuel Pump					
1st stage	16858	637.8	31494	645.5	0.5854
2nd stage	17901	641.0	31494	700.7	0.5686
LOX Pump	1212	199.9	12598	529.1	0.6408

Turbine Pressure Ratio (T-S)	1.402	
Turbine Exit Pressure (static)	580.6	psia
Turbine Exit Temperature	360.9	R
Turbine delta-H	92.02	BTU/lb
Turbine Efficiency	0.7353	
Turbine Torque	1577.8	lbf-in
Veocity Ratio (U/Co)	0.4581	

COOLING JACKET PERFORMANCE

Cooling Jacket delta-P (total)	195.7	psid
Cooling Jacket delta-T	326.3	R
Total Heat Pick-up	7714.2	BTU/sec
Maximum Metal Temp	1500.8	R

VALVE PERFORMANCE

Thrust Control Open Area	.004836	sq.in.
Turbine Bypass Flow	.02634	lb/sec
Oxidizer Control Open Area	.5783	sq.in.
OCV primary flow	28.10	lb/sec
OCV bypass flow	2.659	lb/sec

Table 1
RL10A-3-3A Steady-state Model Output

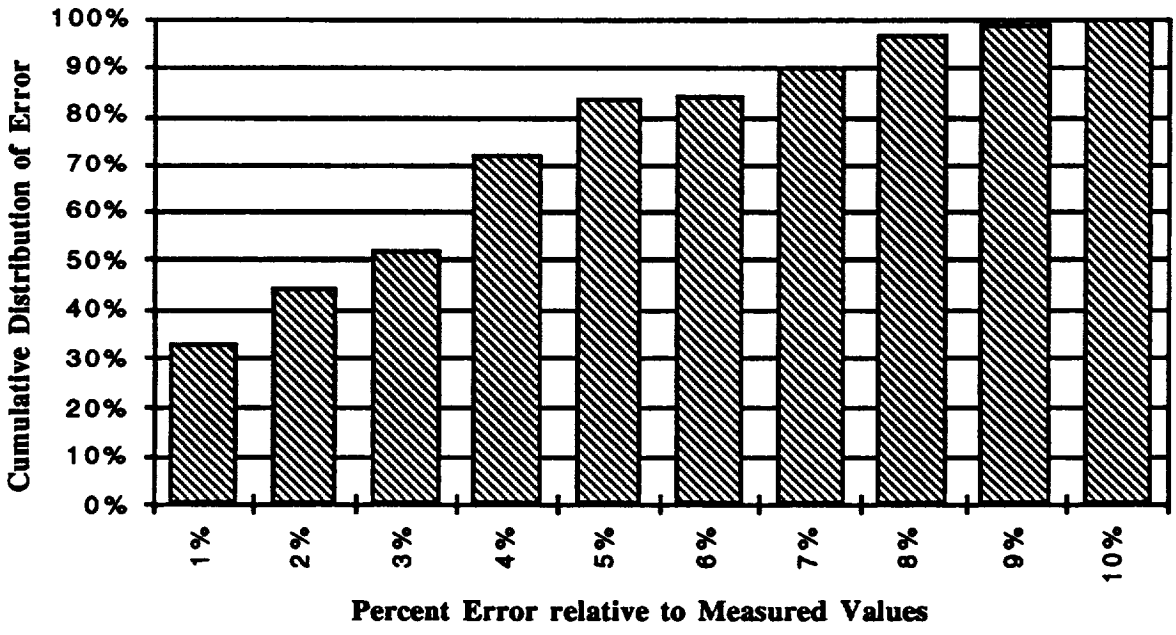

Figure 7
Steady-state Predictions vs. Measurements from Ground-Test Engine Runs (all runs, all parameters)

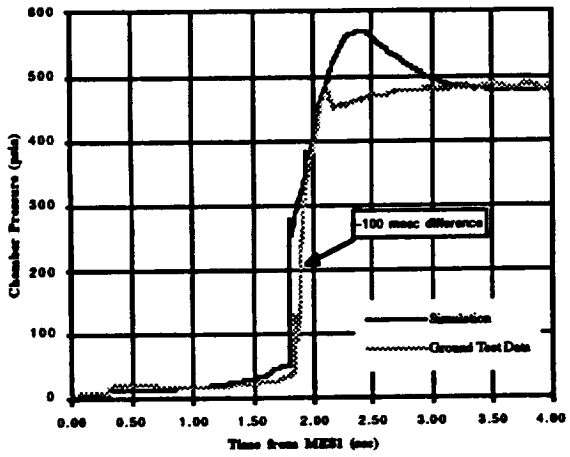

(a)

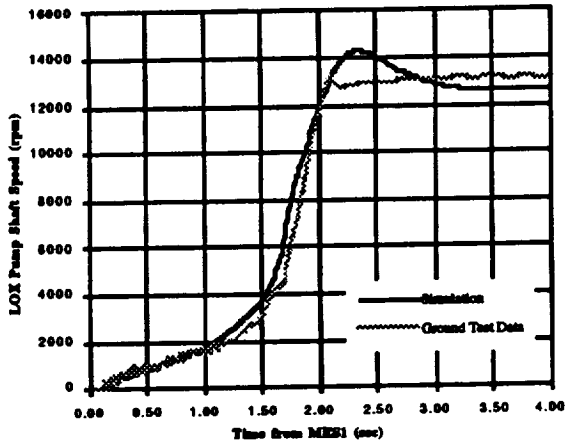

(b)

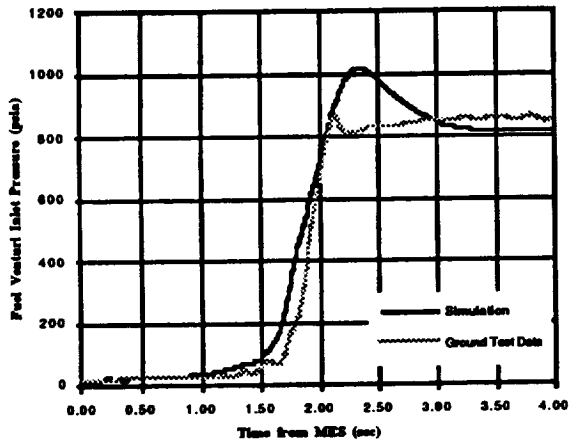

(c)

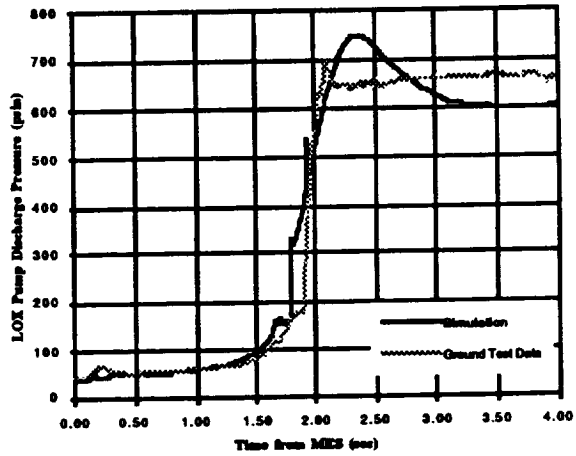

(d)

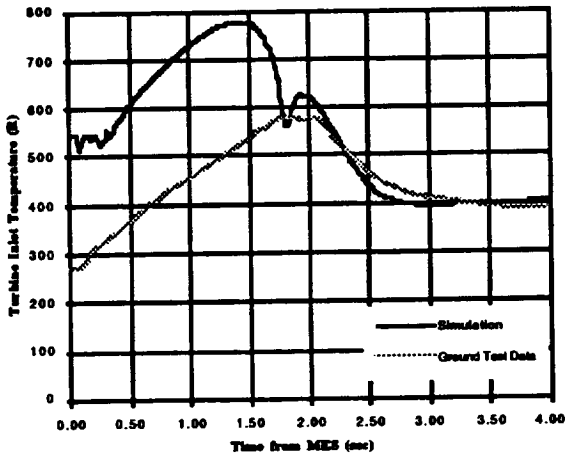

(e)

Figure 8
RL10A-3-3A Start Transient Simulation Output for Ground Test Conditions

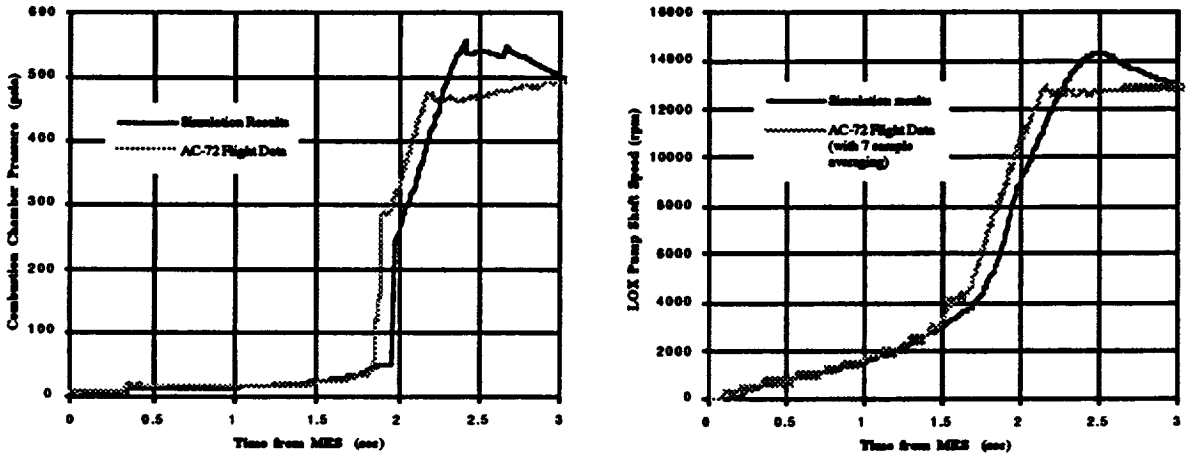

Figure 9
RL10A-3-3A Start Transient Simulation Output
for Atlas/Centaur Flight AC-72 (first burn)

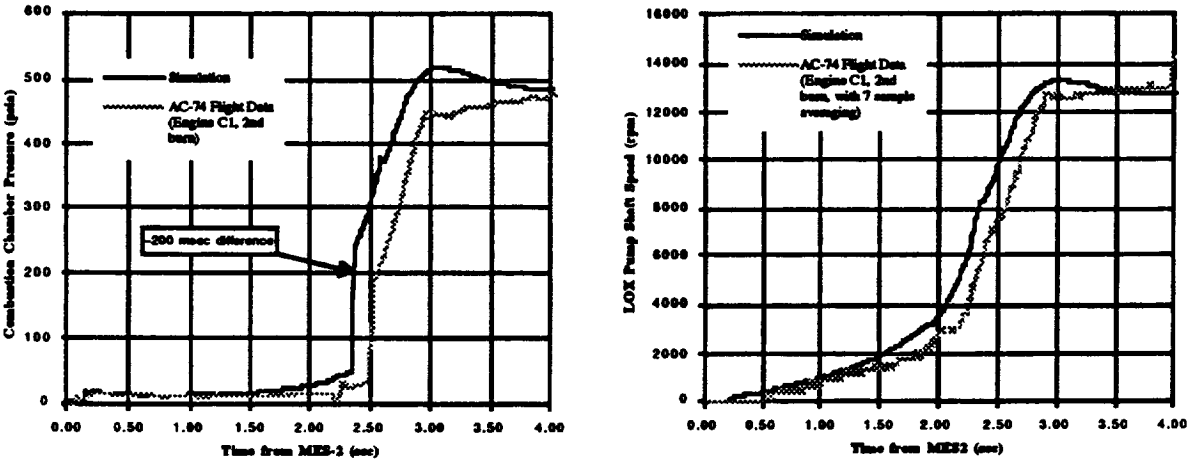

Figure 10
RL10A-3-3A Start Transient Simulation Output
for Atlas/Centaur Flight AC-74 (2nd burn)

Table 2
Comparison of Measured and Predicted
RL10 Engine Time-to-Accelerate

Type of Run	Simulation Time (sec from MES)	Measured Time (sec from MES)	difference (msec)
Ground Test	2.09	2.26	170 (early)
Ground Test	1.80	1.90	100 (early)
Ground Test	1.51	1.43	80 (late)
Ground Test	1.72	1.70	20 (late)
Ground Test (Relight)	1.91	1.84	70 (late)
Ground Test (Relight)	2.00	2.08	80 (early)
Flight	1.98	1.90	80 (late)
Flight	1.95	1.67	280 (late) *
Flight (Relight)	2.33	2.56	230 (early)

* Note : Although this run had inlet conditions similar to other flights, these engines started about 300 msec earlier relative to MES. This may indicate a difference in the engine other than inlet conditions (see section of this report on uncertainty).

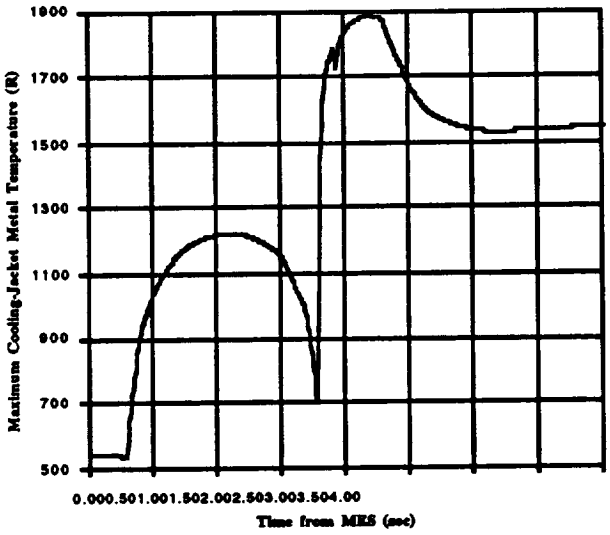

Figure 11
Predicted Maximum Cooling Jacket Metal Temperature during Engine Start

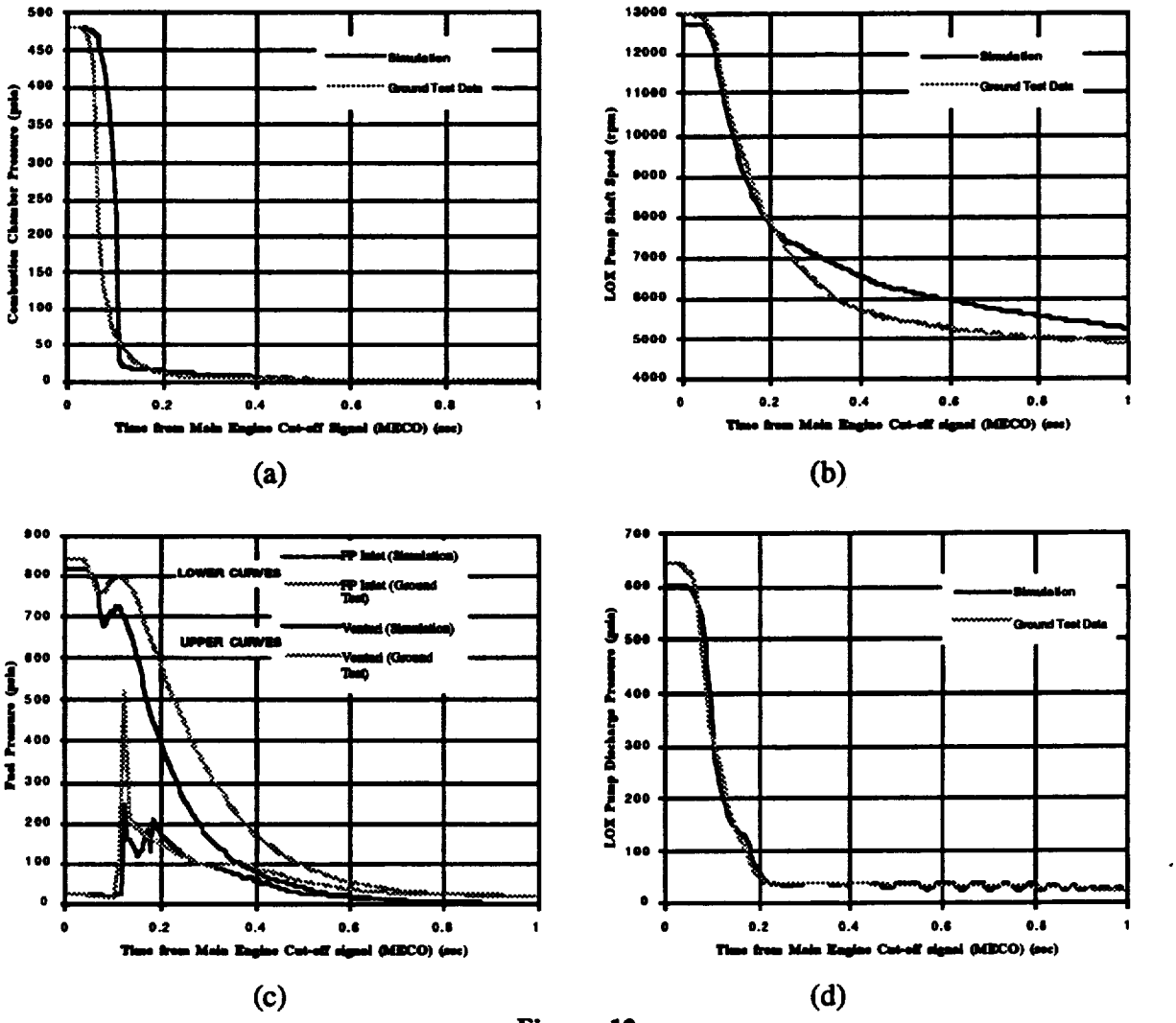

Figure 12
RL10A-3-3A Shutdown Simulation for Ground Test Conditions

REPORT DOCUMENTATION PAGE

Form Approved
OMB No. 0704-0188

1. AGENCY USE ONLY (Leave blank)	2. REPORT DATE	3. REPORT TYPE AND DATES COVERED
	June 1995	Final Contractor Report

4. TITLE AND SUBTITLE
A Transient Model of the RL10A-3-3A Rocket Engine

5. FUNDING NUMBERS
WU-242-70-04
C-NAS3-27186

6. AUTHOR(S)
Michael P. Binder

7. PERFORMING ORGANIZATION NAME(S) AND ADDRESS(ES)
NYMA, Inc.
Engineering Services Division
2001 Aerospace Parkway
Brook Park, Ohio 44142

8. PERFORMING ORGANIZATION REPORT NUMBER
E-9702

9. SPONSORING/MONITORING AGENCY NAME(S) AND ADDRESS(ES)
National Aeronautics and Space Administration
Lewis Research Center
Cleveland, Ohio 44135-3191

10. SPONSORING/MONITORING AGENCY REPORT NUMBER
NASA CR-195478
AIAA-95-2968

11. SUPPLEMENTARY NOTES
Prepared for the 31st Joint Propulsion Conference and Exhibit, cosponsored by AIAA, ASME, SAE, ASEE, San Diego, California, July 10-12, 1995. Project manager, Joseph A. Hemminger, Space Propulsion Technology Division, NASA Lewis Research Center, organization code 5320, (216) 433-7563.

12a. DISTRIBUTION/AVAILABILITY STATEMENT
Unclassified - Unlimited
Subject Category 20

This publication is available from the NASA Center for Aerospace Information, (301) 621-0390.

12b. DISTRIBUTION CODE

13. ABSTRACT *(Maximum 200 words)*

RL10A-3-3A rocket engines have served as the main propulsion system for Centaur upper stage vehicles since the early 1980's. This hydrogen/oxygen expander cycle engine continues to play a major role in the American launch industry. The Space Propulsion Technology Division at the NASA Lewis Research Center has created a computer model of the RL10 engine, based on detailed component analyses and available test data. This R10 engine model can predict the performance of the engine over a wide range of operating conditions. The model may also be used to predict the effects of any proposed design changes and anticipated failure scenarios. In this paper, the results of the component analyses are discussed. Simulation results from the new system model are compared with engine test and flight data, including the start and shut-down transient characteristics.

14. SUBJECT TERMS	15. NUMBER OF PAGES
RL10; RL10A3-3A; Centaur; Transient system model; ROCETS Program	22
	16. PRICE CODE: A03

17. SECURITY CLASSIFICATION OF REPORT	18. SECURITY CLASSIFICATION OF THIS PAGE	19. SECURITY CLASSIFICATION OF ABSTRACT	20. LIMITATION OF ABSTRACT
Unclassified	Unclassified	Unclassified	

National Aeronautics and
Space Administration

Lewis Research Center
21000 Brookpark Rd.
Cleveland, OH 44135-3191